Electronic Supplementary Material (ESI) for Green Chemistry.

Supporting information

Low temperature and high-power density lignin flow fuel cell via efficient CoMn-LDH electrocatalyst with super-hydrophilic intercalation

Tengda Liang,[a] Xihong Zu,*[a,b] Bowen Liu,[a] Xueqing Qiu,*[a,b] Zixin Xie,[a] Xiaofei Wang [a] and Dongjie Yang [c]

[a] *Guangdong Provincial Key Laboratory of Plant Resources Biorefinery, School of Chemical Engineering and Light Industry, Guangdong University of Technology, Guangzhou, Guangdong, 510006, P. R. China*

[b] *Guangdong Provincial Laboratory of Chemistry and Fine Chemical Engineering Jieyang Center, Jieyang 515200, China*

[c] *Guangdong Provincial Key Laboratory of Fuel Cell Technology, School of Chemistry and Chemical Engineering, South China University of Technology, Guangzhou, Guangdong, 510640, P.R. China*

***Corresponding authors:** Prof. Xihong Zu, Prof. Xueqing Qiu

E-mail address: xhzu@gdut.edu.cn (X. Zu); cexqqiu@scut.edu.cn (X. Qiu).

1. Experimental Section

Chemicals: Ammonium fluoride (NH_4F, 98%), urea (99%), cobalt nitrate hexahydrate (99%) and sodium hydroxide (99%) were all from Aladdin Industrial Corporation. Manganese nitrate hexahydrate (99%) was from Macklin Biochemical Co., Ltd (Shanghai, China). Vanadium oxide (V_2O_5, 99. 6%) was from Thermo Fisher. Nitric acid (HNO_3, 65%~68%) and sulfuric acid (H_2SO_4, 98.3%) were all from Guangzhou Chemical Reagent (Guangzhou, China). Enzymatic hydrolysis lignin, alkali lignin and sodium lignosulfonate were ordered from Shandong Longli Biotechnology Co., ltd (Shandong, China). Nafion® 211 membrane was from DuPont. Graphite felt was from Carbon Energy Technology Co., Ltd (Taiwan China).

Preparation of CoMn-LDH nanowire arrays on Graphite felt: In a typical synthesis, 5 mmol $Co(NO_3)_2\cdot 6H_2O$, 2.84 mmol $Mn(NO_3)_2\cdot 4H_2O$, 10 mmol NH_4F and 25 mmol $CO(NH_2)_2$ were dissolved in 70 mL of deionized water and stirred for 10 min to form a homogeneous solution.

Then, the mixture was transferred into a 100 mL teflon-lined stainless steel autoclave containing graphite felt (5 cm × 0.5 cm × 0.5 cm) and hydrothermally treated at 120°C for 5 h. After cooling to room temperature, the prepared sample was washed several times with deionized water and dried in an oven at 60°C overnight to obtain CoMn-LDH on the graphite felt. To investigate the effect of hydrothermal time, we prepare a series of samples using the similar methods with different hydrothermal time.

Preparation of lignin anolyte: The calculated amount of lignin and sodium hydroxide were dissolved in 50 ml deionized water, stir for 10 minutes, and filter out insoluble impurities, and obtain lignin anolyte. The influence of lignin concentration and sodium hydroxide concentration on fuel cell performance were investigated.

Preparation of catholyte: 20 g V_2O_5, 76 ml H_2SO_4 (98.3%) and 4 ml HNO_3 (65%~68%) were dissolved in 524 ml deionized water, then the solution was continuously stirred until it turned into yellow transparent solution.

Assembly of the LFFC and discharging performance measurement: The LFFC consists of two all carbon graphite electrodes with serpentine flow channels, and it was separated by Nafion 211 membrane with a total active area of 1 cm^2. The graphite felt was filled in the cathode flow channel, and the modified graphite felt was filled in the anode flow channel. The anolyte and catholyte were pumped through the LFFC at a flow rate of 10 mL min^{-1}. Oxygen was injected into the catholyte at a flow rate of 40 mL min^{-1} under the catalysis of nitric acid for oxidizing VO^{2+} into VO_2^+, realizing the regeneration of catholyte. The LFFC system was operated at 90°C. The cell performance was tested by the 857 Flow Cell Test System (Scribner Associates Inc., USA). Continuous discharge performance of LFFC tested by the constant voltage discharging method at 0.3 V using a Gamry electrochemical workstation.

Characterization: The morphology of CoMn-LDH/GF was characterized by field emission scanning electron microscopy (FESEM，Hitach SU8220) and TEM (FEI Titan G2 60-300, USA). The Raman spectra were measured with a micro confocal Raman spectrometer (HORIBA Jobin Yvon LabRAM HR Evolution) using a laser excitation wavelength of 532 nm. X-ray diffraction patterns were collected on a D8 Advance X-ray diffractometer (XRD, Bruker, Germany) with a Cu Kα radiation (λ=1.5406 Å). X-ray photoelectron spectroscopy (XPS) was recorded on an Escalab 250Xi X-ray photoelectron spectrometer (Thermo Fisher Scientific) with monochromatic Al Ka radiation (1486.6 eV). The hydrophilicity of electrode was analyzed with Milli-Q water by contact angle tester (Dataphysics, OCA100, Germany). The FTIR spectra were recorded with Full band research grade infrared spectrum workstation (THEMOR-FILSHER, iS50R, USA). QCM-D measurements were performed by an E4 QCM-D equipment

(Q-Sense, Sweden) at 25°C. The detail test procedures are as following. Firstly, the CoMn-LDH and $MnCo_2O_4$ electrocatalysts were both peeled from GF through ultrasound, respectively. Secondly, 10 mg of CoMn-LDH or $MnCo_2O_4$ electrocatalyst was dispersed in 1 ml ethanol, and then uniformly dispersed on the electrode surface of the QCM-D through spin coating. After that, deionized water was pumped into the electrode at a rate of 0.15 mL min^{-1} at 25°C until an equilibrium state appeared, and then the vanillin solution (0.02 g ml^{-1} vanillin and 2 M NaOH) was pumped into the electrode at a rate of 0.15 mL min^{-1} at 25°C to test the adsorbing capacity of vanillin on the CoMn-LDH or $MnCo_2O_4$ electrocatalyst. 2D HSQC NMR spectra and GPC were used to analyze the degradation products and structural changes of lignin before and after discharging. For 2D Heteronuclear single quantum coherence (HSQC) NMR analysis, 30 mg lignin was added to 0.6 mL dimethyl sulfoxide-d6, ultrasound, and transferred to nuclear magnetic tube after complete dissolution. 2D-HSQC NMR spectra of lignin were conducted using a Bruker Advance III 400 MHz spectrometer with 512 scans at room temperature (~25°C). The spectral widths were 5000 and 18000 Hz for the ^1H and ^{13}C dimensions, respectively. The number of collected complex points was 1024 for the ^1H dimension and 256 for the ^{13}C dimension with a recycle delay of 1.5 s and several transients of 32. The average molecular weight change of lignin and oxidation products were analyzed with a Gel permeation chromatography (GPC) system (Agilent GPC-8026 column and an SPD-20A UV detector). Acetylated lignin sample (2 mg) was dissolved in 1 mL of tetrahydrofuran (THF), with THF as the mobile phase, flow rate of 1 ml min^{-1}, and column temperature of 30°C. Use polystyrene with molecular weights ranging from 160 g mol^{-1} to 19880 g mol^{-1} to calibrate the chromatographic column and obtain a standard curve. The vanillin oxidation products were characterized by HPLC-MS (TSQ Endura, Thermo Fisher, USA) and headspace gas chromatography-mass spectroscopy (HS-GC-MS) (Agilent 7890A-5975C) with a WM-624 (60 m × 320 μm × 1.8 μm) capillary column.

DFT calculations: DFT calculations were performed using the Vienna ab initio simulation package (VASP) with the projector augmented wave (PAW) pseudopotentials [1-3]. The generalized gradient approximation with the spin-polarized Perdew-Burke-Ernzerhof (PBE) functional was used to characterize the exchange-correlation potential [4-6]. The electron-ion interaction was described using the projector augmented wave, and the plane-wave energy cutoff was set to 400 eV. The structures were optimized using a convergence criterion of 1×10^{-5} eV for the energy and 0.01 eV/Å for the forces. A periodic 4 × 4 graphene support was also built. The vacuum spacing was set to more than 15 Å for surface isolation to prevent interactions between the two neighboring surfaces. Brillouin zone sampling was employed by using a Monkhorst-Packing grid with 9 × 9 × 1 for the calculated models. Dense k-points (9 × 9 × 1) were used for the calculations of the density of states (DOSs). Geometry optimizations were performed with a 3 × 3 × 1 k-mesh.

2. The reaction principle of LFFC

When the CoMn-LDH was employed as electrocatalyst, the reaction principle of LFFCs includes three parts. Firstly, the oxidation of lignin takes place in the anodic compartment catalyzed by CoMn-LDH.

$$lignin - H_n + nOH^- - ne^- \xrightarrow{CoMn-LDH} Oxidized\,products + nH_2O \tag{1}$$

Secondly, VO_2^+ receives electrons from the external circuit and is reduced to VO^{2+} in the cathode chamber.

$$VO_2^+ + 2H^+ + e^- \rightarrow VO^{2+} + H_2O \tag{2}$$

Finally, O_2 is introduced into the cathode electrolyte to oxidize VO^{2+} ions into VO_2^+ under the catalysis of nitric acid to maintain a high electrical potential for stable power output.

$$4VO^{2+} + O_2 + 2H_2O \xrightarrow{HNO_3} 4VO_2^+ + 4H^+ \tag{3}$$

3. Supplementary Figures

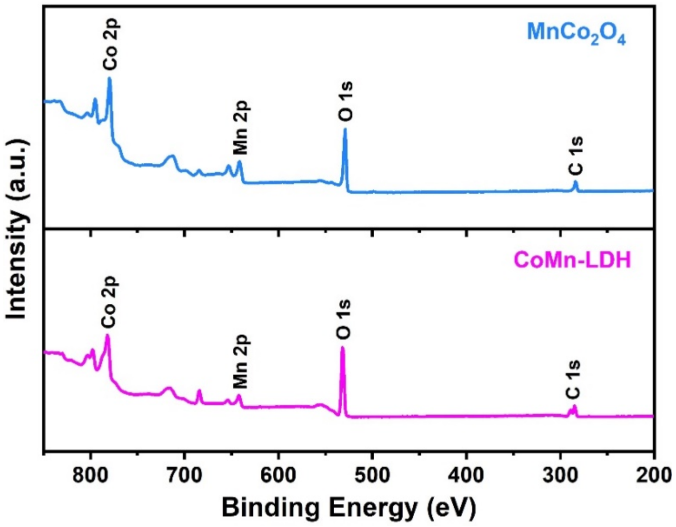

Fig. S1. XPS full spectrum of CoMn-LDH and $MnCo_2O_4$

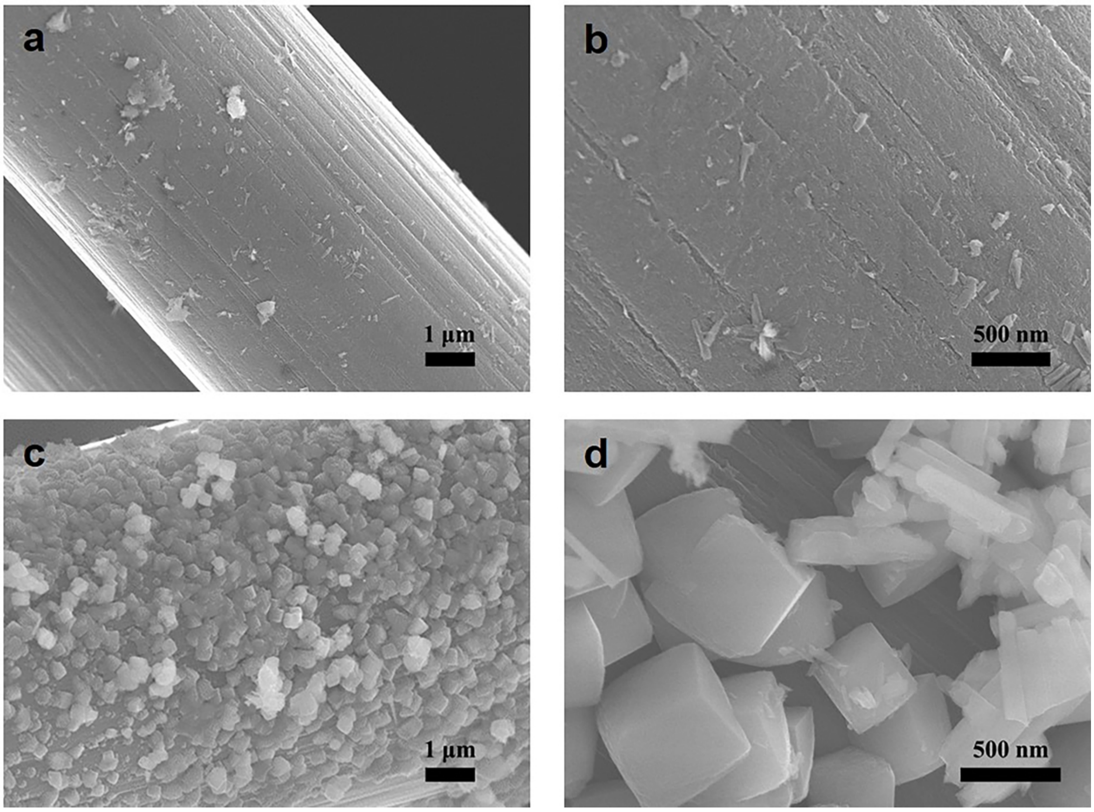

Fig. S2. SEM images of CoMn-LDH by hydrothermal reaction with different times. (a-b) 1 h, (c-d) 3 h.

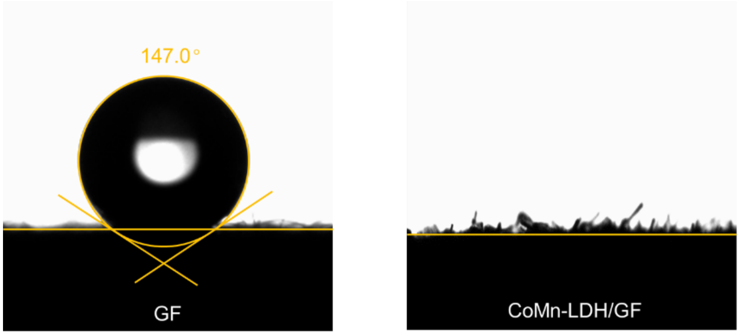

Fig. S3. Water contact angles of the GF and CoMn-LDH/GF.

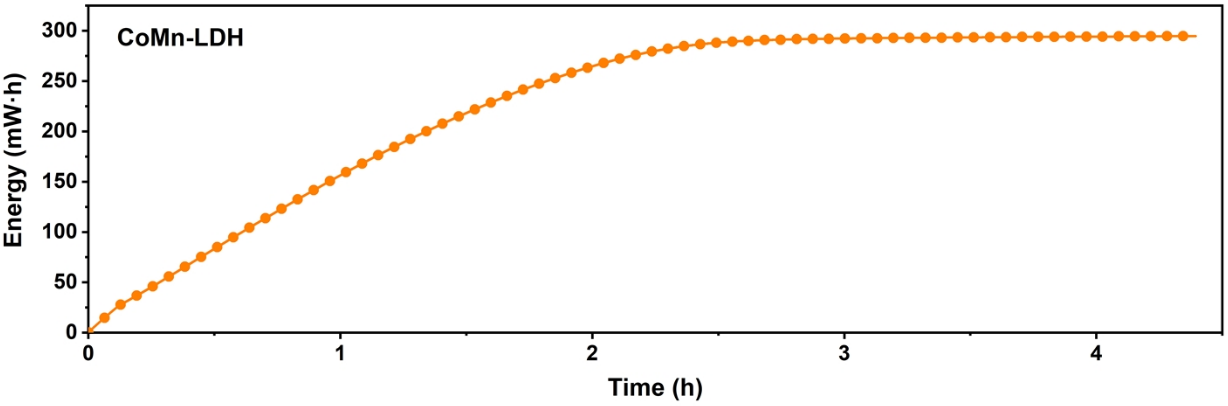

Fig. S4. Output energy of the LFFC tested by the constant voltage discharging method at 0.3 V (100 mL solution containing 1 g enzymatic hydrolysis lignin and 2 M NaOH).

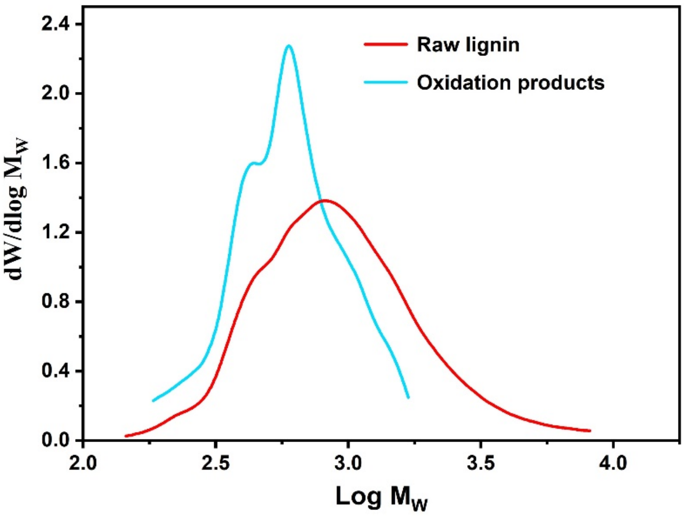

Fig. S5. GPC chromatograms of raw enzymatic hydrolysis lignin and oxidation products after discharging 9 h.

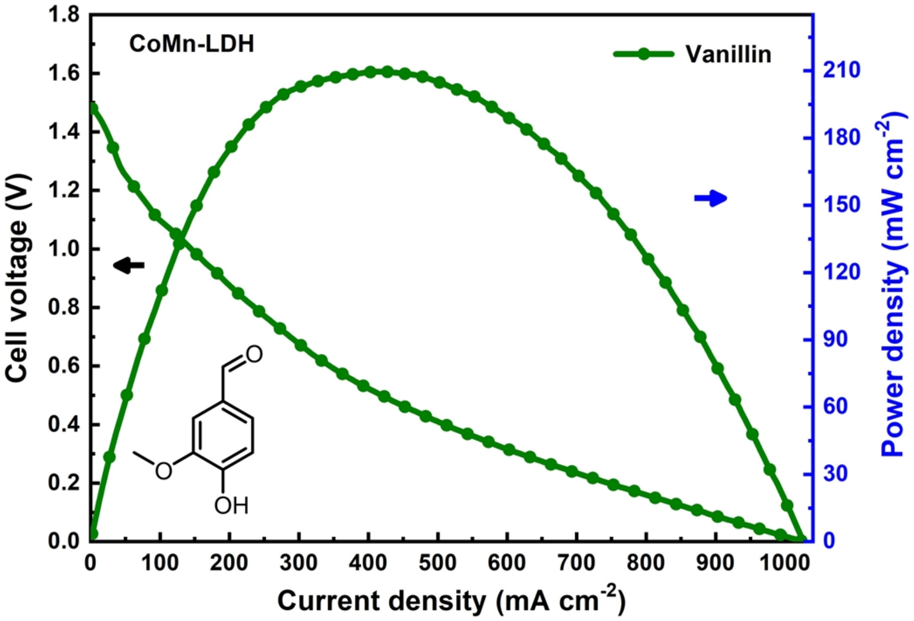

Fig. S6. I-V/I-P curves of LFFC with vanillin as fuel.

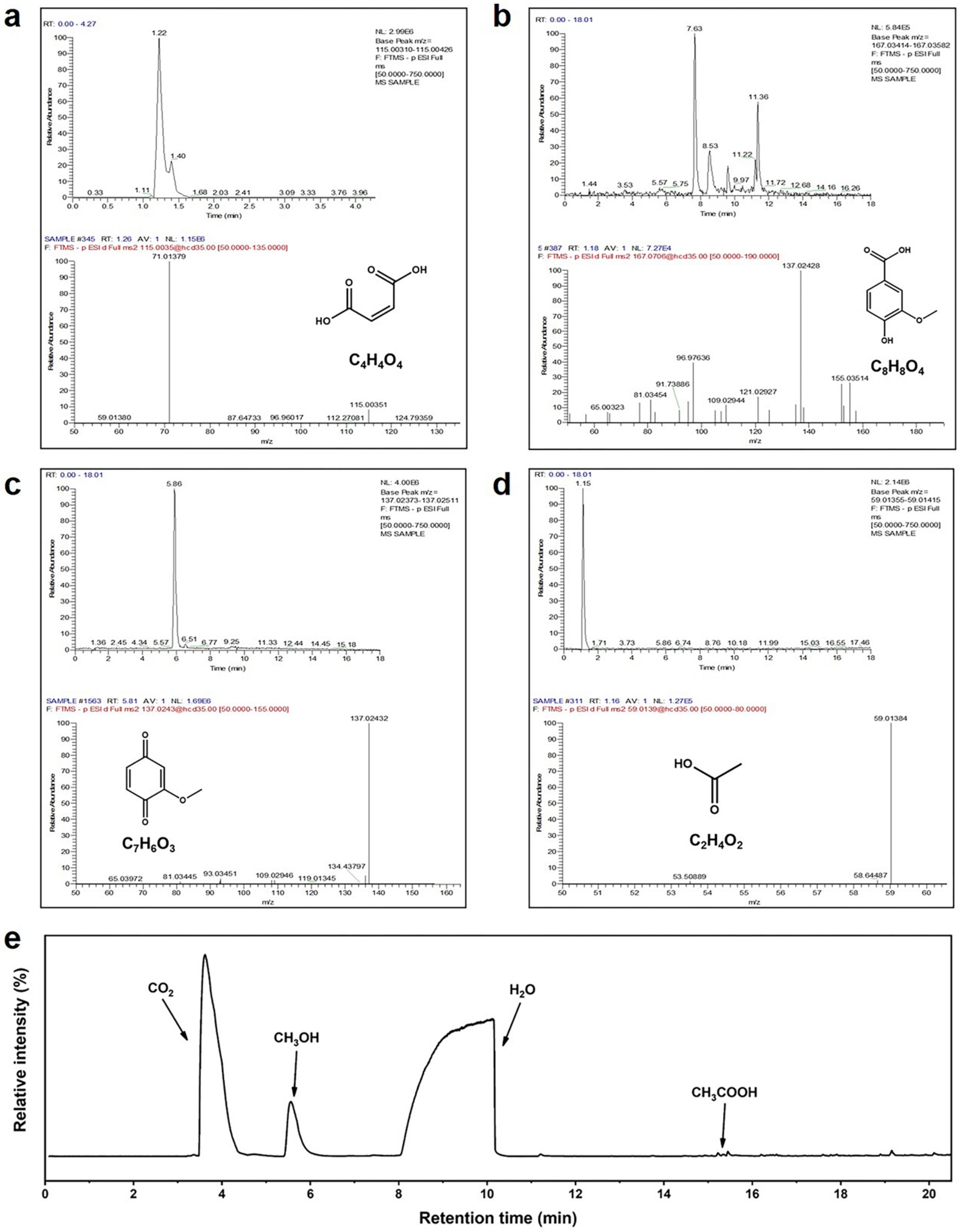

Fig. S7. Qualitative HPLC-MS spectra (a-d) and HS-GC-MS (e) of vanillin after discharging 2 h by using CoMn-LDH/GF as electrocatalyst. Note: The initial anolyte was 50 mL solution containing 1 g vanillin with 2 M NaOH.

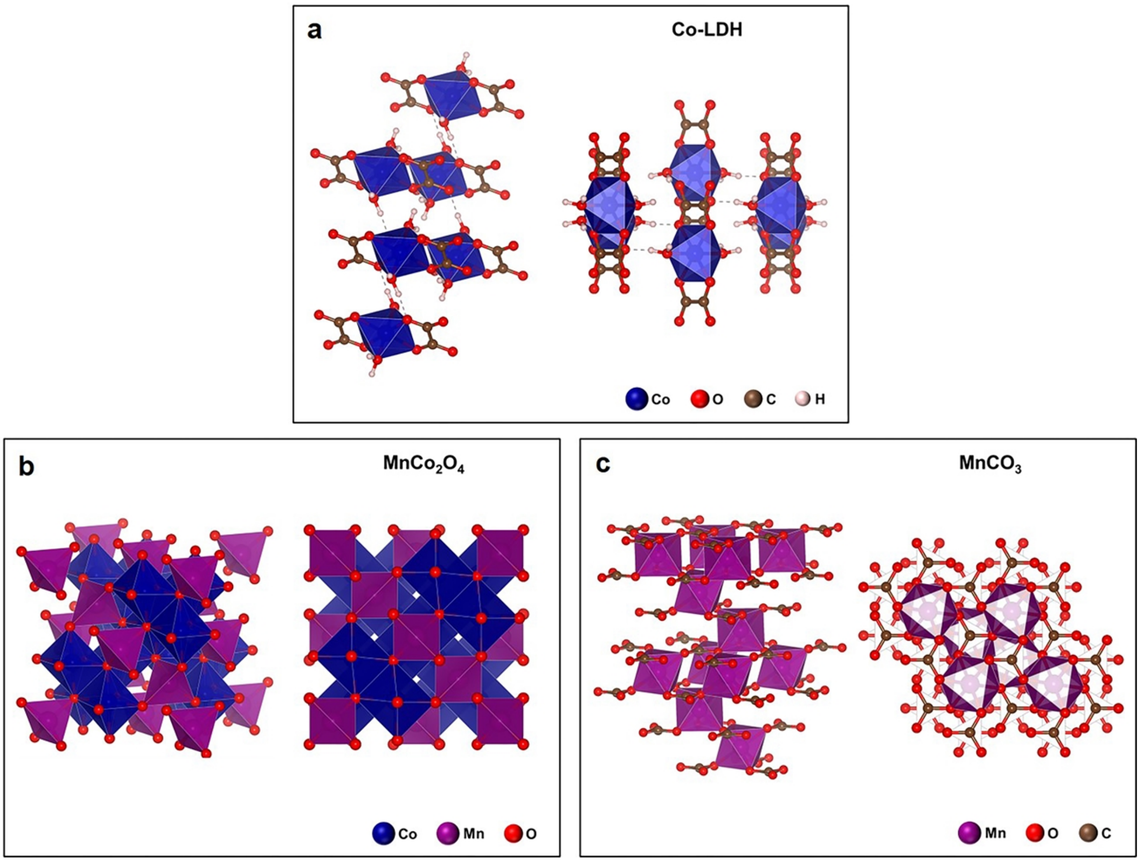

Fig. S8. Crystal structure (polyhedral model) of (a) Co-LDH, (b) $MnCo_2O_4$, (c) $MnCO_3$.

4. Supplementary Tables

Table S1. Elemental compositions of CoMn-LDH by ICP-MS

Sample	Atomic content	Metal weight percentage		
	M_{Mn}/M_{Co} Ratio	M_{Mn} (wt %)	M_{Co} (wt %)	Total metal (wt %)
CoMn-LDH	0.49 （1：2）	11.26	24.39	35.65

Table S2. Assignments of main ^{13}C-^{1}H cross-signals in the 2D HSQC NMR spectra of the lignin samples

Label	δC/δH (~ppm)	assignment
-OMe	55.6/3.73	C-H in methoxyls
A_α	72.4/4.96	C_γ-H_γ in β-O-4′ substructures (A)
A_β	86.2/4.25	C_β-H_β in β-O-4′ substructures linked to S units (A)
A_β	84.5/4.50	C_β-H_β in β-O-4′ substructures linked to G units (A)
A_γ	59.9/3.35-3.8	C_γ-H_γ in β-O-4′ substructures (A)
B_α	86.8/5.48	C_α-H_α in phenylcoumaran substructures (B)
B_β	54.1/3.41	C_β-H_β in phenylcoumaran substructures (B)
B_γ	62.3/3.76	C_γ-H_γ in phenylcoumaran substructures (B)
C_α	84.8/4.65	C_α-H_α in β-β resinol substructures (C)
C_β	5.26/3.13	C_β-H_β in β-β resinol substructures (C)
C_γ	71.0/3.79-4.18	C_γ-H_γ in β-β resinol substructures (C)
Gly_α	73.0/4.45	C_α-H_α in arylglycerol substructures (Gly)
Gly_β	75.5/3.48	C_β-H_β in arylglycerol substructures (Gly)
Gly_γ	62.3/3.16-3.36	C_γ-H_γ in arylglycerol substructures (Gly)
$S_{2,6}$	104.1/6.71	$C_{2,6}$-$H_{2,6}$ in etherified syringyl units (S)
$S'_{2,6}$	112.2/7.39	$C_{2,6}$-$H_{2,6}$ in oxidized syringyl units (S’)
G_2	111.2/7.29	C_2-H_2 in guaiacyl units (G)
G_5	114.9/6.77	C_5-H_5 in guaiacyl units (G)
G_6	119.7/6.75	C_6-H_6 in guaiacyl units (G’)
G'_2	112.3/7.32	C_2-H_2 in oxidized guaiacyl units (G)
$H_{2,6}$	127.7/7.19	$C_{2,6}$-$H_{2,6}$ in p-hydroxyphenyl units (H)
PCA_α and FA_α	144.6/7.45	C_α-H_α in p-coumarate (PCA) and ferulate (FA)
PCA_β and FA_β	115.5/6.29	C_β-H_β in p-coumarate (PCA) and ferulate (FA)
$PCA_{3,5}$	115.5/6.29	$C_{2,6}$-$H_{2,6}$ in p-coumarate (PCA)
FA_2	114.9/7.41	C_2-H_2 in ferulate (FA)
FA_6	123.8/7.20	C_6-H_6 in ferulate (FA)
$SB_{5\alpha}$	128.2/7.07	C_α-H_α in β-5 substructures (SB_5)
$SB_{5\beta}$	120.1/7.22	C_β-H_β in β-5 substructures (SB_5)

Table S3. Comparison of different lignocellulose fuel cells

Fuel Cell Type	Fuels	Redox mediators or catalyzer	Peak power density	Operating temp.	Ref.
MFC	Barley straw	Shewanella marisflavi BBL25	52.80 mW cm^{-2}	30℃	Journal of Cleaner Production 2020, 277, 124084
MFC	Miscanthus sacchariflorus	Escherichia coli	0.0963 mW cm^{-2}	37℃	Journal of Cleaner Production 2022, 361, 132269
SOFC	Alkali lignin	Fe_2O_3	450 mW cm^{-2}	800℃	ACS Sustainable Chemistry & Engineering 2021, 9, 8, 3124-3136
SO-DCFC	Rice husk	-	135 mW cm^{-2}	850℃	International Journal of Energy Research 2022, 46, 4965-4974
SO-DCFC	Rice husk	-	66.9 mW cm^{-2}	750℃	International Journal of Energy Research 2022, 46, 9822-9835
SO-DCFC	Solidago canadensis	Ag-Fe_2O_3	410 mW cm^{-2}	800℃	Electrochimica Acta 2021, 388, 138681
LFFC	Sodium lignosulfonate	$CuCl_2$/$TiOSO_4$	55.1 mW cm^{-2}	90℃	Chemical Engineering Journal 2023, 452, 139266
LFFC	Sugarcane bagasse	$FeCl_3$	54.5 mW cm^{-2}	90℃	Journal of Power Sources 2020, 448, 227441
LFFC	corn stover	$K_3[Fe(CN)_6]$	139.9 mW cm^{-2}	90℃	Energy Conversion and Management 2022, 258, 115552
LFFC	wheat straw	Methylene blue	41.8 mW cm^{-2}	90℃	Applied Catalysis B: Environmental 2020, 265, 118578
LFFC	wheat straw	$H_4PMo_9V_3O_{40}$	44.7 mW cm^{-2}	90℃	Journal of Energy Chemistry 2021, 58, 133-146
LFFC	bagasse	$FeCl_3$	45.1 mW cm^{-2}	90℃	Chemical Engineering Journal 2018, 348, 476-484
LFFC	Enzymatic hydrolysis lignin	-	159.9 mW cm^{-2}	90℃	Green Chemistry 2024, 26, 2021
LFFC	Enzymatic hydrolysis lignin	CoMn-LDH	269.3 mW cm^{-2}	90℃	This work

Note: MFC means microbial fuel cell; SOFC means solid oxide fuel cell; SO-DCFC means solid oxide direct carbon fuel cell; LFFC means liquid flow fuel cell.

Table S4. GPC results of enzymatic hydrolysis lignin before and after 9 h discharge

Sample	Number average Mn	Weight average Mw	PDI
Raw lignin	797	2452	3.08
After 9 h of reaction	681	1113	1.63

Table S5. Comparison of the generated electric energy of different biomass flow fuel cells based on 1.0 g biomass.

Fuel cell types	**Fuels in anode half-cell**	**Redox mediators in anolyte**	**Redox mediators in catholyte**	**External processing or pretreatment**	**Electric energy (mW h)**	**Ref.**
BFFC	Wheat straw	PMo_9V_3	$FeCl_3$	The suspension was heated in an autoclave at 120℃ for 1 h.	24.6	7
BFFC	Sugarcane bagasse	$FeCl_3$	$FeCl_3$	The suspension was heated in an autoclave at 120℃ for 30 min.	101.4	8
BFFC	Sugarcane bagasse	$K_3[Fe(CN)_6]$	$FeCl_3$	The suspension was heated in an autoclave at 120℃ for 30 min.	28.9	8
LFFC	Sodium lignosulfonate	$CuCl_2/TiOSO_4$	$(VO_2)_2SO_4$	The solution was heated to 90℃ under stirring to react 1 h.	116.24	9
LFFC	Alkali lignin	None	$(VO_2)_2SO_4$	None	219.9	10
LFFC	Enzymatic hydrolysis lignin	None	$(VO_2)_2SO_4$	None	294.7	This Work

Supplementary References

[1] Kresse, G. & Furthmüller, J. Efficiency of ab-initio total energy calculations for metals and semiconductors using a plane-wave basis set. Comput. Mater. Sci. 1996, 6, 15-50.

[2] Kresse, G. & Furthmüller, J. Efficient iterative schemes for ab initio total-energy calculations using a plane-wave basis set. Phys. Rev. B. 1996, 54, 11169-11186.

[3] Kresse, G. & Hafner, J. Ab initio molecular-dynamics simulation of the liquid-metal-amorphous-semiconductor transition in germanium. Phys. Rev. B. 1994, 49, 14251-14269.

[4] Kresse, G. & Joubert, D. From ultrasoft pseudopotentials to the projector augmented-wave method. Phys. Rev. B. 1999, 59, 1758-1775.

[5] Blöchl, P. E. Projector augmented-wave method. Phys. Rev. B. 1994, 50, 17953-17979.

[6] Perdew, J. P., Burke, K. & Ernzerhof, M. Generalized gradient approximation made simple. Phys. Rev. Lett. 1996, 77, 3865-3868.

[7] H. Yang, Y. Bai, D. Ouyang, F. Wang, D. Liu, X. Zhao, J. Energy Chem., 2021, 58, 133-146.

[8] D. Ouyang, Y. Han, F. Wang, X. Zhao, Bioresour. Technol., 2022, 344, 126189.

[9] C. She, X. Zu, Z. Yang, L. Chen, Z. Xie, H. Yang, D. Yang, G. Yi, Y. Qin, X. Lin, Chem. Eng. J., 2023, 452, 139266.

[10] Z. Xie, X. Zu, J. Lin, X. Qiu, T. Liang, L. Chen, Green Chem. 2024, 26, 2021.